UCLouvain
Institute of Mechanics,
Materials and Civil Engineering

Robust optimisation of the pathway towards a sustainable whole-energy system

A hierarchical multi-objective reinforcement-learning based approach

Doctoral dissertation presented by
Xavier RIXHON
in partial fulfillment of the requirements for
the degree of Doctor in Engineering Sciences

December 2023

Thesis committee
Pr. Francesco CONTINO (supervisor, UCLouvain)
Pr. Hervé JEANMART (supervisor, UCLouvain)
Dr. Stefano MORET (ETH Zurich)
Pr. Sylvain QUOILIN (ULiège)

Contents

Symbols

Acronyms

API	application programming interface
BECCS	bioenergy with carbon capture and storage
BEMS	building energy management system
BEV	battery electric vehicle
BTX	benzene, toluene and xylene
CAPEX	capital expenditure
CCGT	combined cycle gas turbine
CCS	carbon capture and storage
CHP	combined heat and power
CNG	compressed natural gas
DC	direct current
DHN	district heating network
DNN	deep neural network
DRL	deep reinforcement learning
ESOMs	energy system optimisation models
EnergyScope TD	EnergyScope Typical Days
EUD	end-use demand
FC	fuel cell
FEC	final energy consumed
GDP	gross domestic product
GHG	greenhouse gases
GSA	global sensitivity analysis
GWP	global warming potential
HP	heat pump
HT	high-temperature

HVC	high value chemicals
IAMs	integrated assessment models
ICE	internal combustion engine
IEA	International Energy Agency
IPCC	intergovernmental panel on climate change
IQR	interquatile range
LCA	life cycle assessment
LCOE	levelised cost of energy
LFO	light fuel oil
LOO	leave-one-out
LP	linear programming
LPG	liquefied petroleum gas
LT	low-temperature
MDP	Markov decision process
MMSA	Methanol Market Services Asia
MTBE	methyl tert-butyl ether
MTO	methanol-to-olefins
NED	non-energy demand
NG	fossil gas
NN	neural network
NRE	non-renewable energy
NSC	naphtha steam cracker
OPEX	operational expenditure
PC	principal component
PCs	principal components
PCA	Principal Component Analysis
PCE	Polynomial Chaos Expansion
PDF	probability density function
PV	photovoltaic
RE	renewable energy
RL	reinforcement learning
SAC	Soft Actor Critic
SDGs	Sustainable Development Goals
SMR	small modular reactor
SVD	singular value decomposition
UQ	uncertainty quantification
VRES	variable renewable energy sources

List of publications

Limpens, G., **Rixhon, X.**, Contino, F., & Jeanmart, H. (2024). "*EnergyScope Pathway: An open-source model to optimise the energy transition pathways of a regional whole-energy system.*" In Applied Energy, (Vol. 358). URL: `https://doi.org/10.1016/j.apenergy.2023.122501`

Rixhon, X., Limpens, G., Coppitters, D., Jeanmart, H.,& Contino, F.(2022). "*The role of electrofuels under uncertainties for the Belgian energy transition.*" In Energies (Vol. 14). URL: `https://doi.org/10.3390/en14134027`

Rixhon, X., Tonelli, D., Colla, M., Verleysen, K., Limpens, G., Jeanmart, H. ,& Contino, F.(2022). "*Integration of non-energy among the end-use demands of bottom-up whole-energy system models.*" In Frontiers in Energy Research, Sec. Process and Energy Systems Engineering, (Vol. 10). URL: `https://doi.org/10.3389/fenrg.2022.904777`

Rixhon, X., Colla, M., Tonelli, D., Verleysen, K., Limpens, G., Jeanmart, H., & Contino, F.(2021). "*Comprehensive integration of the non-energy demand within a whole-energy system: Towards a defossilisation of the chemical industry in Belgium.*" In proceedings of ECOS 2021 conference (Vol. 34, p. 154).

Rixhon, X., Limpens, G., Contino, F., & Jeanmart, H. (2021). "*Taxonomy of the fuels in a whole-energy system.*" In Frontiers in Energy Research, Sec. Sustainable Energy Systems, (Vol. 9). URL: `https://doi.org/10.3389/fenrg.2021.660073`

Limpens, G., Coppitters, D., **Rixhon, X.**, Contino, F., & Jeanmart, H. (2020). "*The impact of uncertainties on the Belgian energy system: application of the Polynomial Chaos Expansion to the EnergyScope model.*" In proceedings of ECOS 2020 conference (Vol. 33, p. 711).

Chapter 1

Robustness assessment of pathway roadmaps

"The more data we have, the more likely we are to drown in it."
Nassim Nicholas Taleb, in *Fooled by Randomness: The Hidden Role of Chance in Life and in the Markets*, 2008

Assessing the robustness of a roadmap driving the transition pathway of a whole-energy system is complex, especially due to the curse of dimensionality. This curse comes from the number of variables of the system (e.g. the installed capacity of technologies), the multiple-year approach specific to the pathway optimisation (i.e. versus the snapshot approach) or the number of uncertain parameters. On top of this, the sector coupling interconnecting the installed capacities and the used resources among the different (non-)energy sectors can make harder the understanding of big trends of such a system. To navigate through this load of uncertain and interconnected data, it is necessary to assess the robustness of pathway roadmaps.

To deal with such uncertainties, decision-makers have several options: (i) resistance; (ii) resilience; (iii) static robustness; and (iv) adaptive robustness [1]. Where resistance consists in planning for the worst-case scenario, resilience aims at a fast recovery whatever the conditions in the future. Finally, in static robustness, one seeks for a roadmap that would perform "satisfactorily" in a wide range of plausible futures, whereas, a roadmap would be dynamically robust if it is prepared to adapt in case of a change in conditions. Where the adaptability of the policy was addressed in Chapter **??**, the objective of this chapter is to apply the method described in Section **??** to deal with the static robustness of pathway roadmaps. Castrejon-Campos et al. [2] assessed policy mix folllowing the same philosophy of “satisfactory level of performance” as [1]. In their work, they mostly focused on the electricity sector, accounting for a variety of stakeholders and related interests using STET (Socio-Technical Energy Transition) models to capture more properly societal and behavioral aspects in relation with policy implementation, enriching purely techno-economy model, like EnergyScope, that usually assume rational choice within an overall cost minimization. However, in the case of the transition pathway of a whole-eenrgy system, the challenges stand here in the definition of the “performance metric” as well as the “satisfactory level of performance”. Between the sole total transition cost and the entire set of installed technologies that give too few and too much information, respectively, the performance metric here is defined through the Principal Component Analysis (PCA) approach. Then, when comes the “satisfactory level of performance”, we propose a relative level of performance through a comparative analysis of different roadmaps. In other terms, one roadmap will not be robust or not in itself but rather more or less robust than another one.

Contributions

The main contributions of this chapter is the application of the methodology proposed in Section **??** to the case study of the Belgian energy transition. First, we develop the different steps that lead to the principal components of the transition. We analyse these big trends of variation and highlight the fact that these variations stand for the entire pathway, a group of consecutive representative years or rather on a tipping-year. Then, and most importantly, we assess the robustness of different technological roadmaps by projecting their resulting myopic pathway against these directions of variation. The application of PCA to provide a new metric for robustness applied to the case of Belgium is the added-value of this chapter.

1.1 Definition of the principal components of the transition

As detailed in Section **??**, we have decided to define the directions of variation, i.e. the robustness metrics, based on the installed capacities through the transition in the different end-use sectors, i.e. electricity, high-temperature (HT) heat, low-temperature (LT) heat, passenger mobility, freight mobility, high value chemicals (HVC), ammonia and methanol. These capacities represent the technological roadmaps to supply these end-use demand (EUD) while respecting the CO_2-budget. As introduced in Section **??**, the data considered in this method come from the global sensitivity analysis (GSA) carried out on the perfect foresight optimisation of the Belgian transition pathway (see Chapter **??**). This gave 1260 different transitions resulting, for each of them, from the pathway optimisation subject to a sample of uncertain parameters (see Section **??**). Appendix A.3 gives the exhaustive distributions of the installed capacities among the different end-use sectors from the GSA.

1.1.1 Principal components of each representative year

After the pre-preprocessing of the raw data (i.e. data scaling and outliers management, see Section **??**), the principal components (PCs) of each representative year of the transition, except 2020 as the initialisation year, can be computed.

First of all, before investigating the PCs, it is worth looking at the total variance of each representative year (see Table 1.1). Even though the absolute value of these variances has no physical meaning, we observe that the variations are more important at earlier stages of the transition. In other words, the further goes the transition, the more limited are the degrees of freedom to respect the CO_2-budget.

Table 1.1. Whole-system design variance of the different representative years and their comparison with 2025.

Year	**Design variance** $[10^{-3}]$	**vs. 2025**
2025	10.4	-
2030	12.1	+15%
2035	9.7	-7%
2040	6.1	-42%
2045	5.1	-51%
2050	4.8	-54%

Then, keeping the PCs capturing at least 90% of the total variance of each representative year, this gives between four, in 2035, and seven, in 2050, PCs depending on the year (see Figure 1.1), and a total of 34 PCs. At later stages of the transition, the increasing number of required PCs, in line with their smaller share of explained variance, is another indication that the variance of the system design is more spread over a wider range of technologies and with a more limited amplitude.

Finally, we consider the respective contribution of the different technologies in the different PC_y, i.e. their corresponding component in the different eigenvectors. Highlighting the top-5 technologies for $PC_{y,1}$, $PC_{y,2}$ and $PC_{y,3}$, we observe general trends over the whole transition as well as tipping year where there is a clear trade-off between several technologies (see Figure 1.2). As pointed out in Section **??**, PCA does

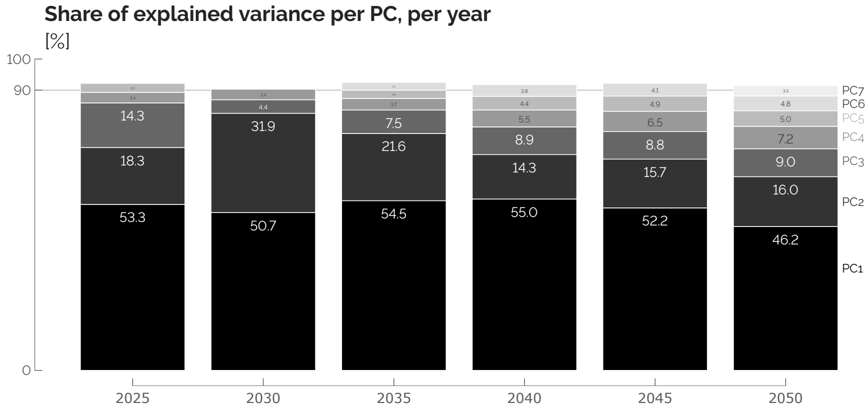

Figure 1.1. PCs capturing at least 90% of the total variance of their respective representative year of the transition.

not make any distinction between a vector of variation and its opposite. This is why $PC_{2025,1}$ and $PC_{2035,1}$ are actually very similar even though there are mostly on the opposite sides of the 0-axis.

Even though the following observations could be made by analysing the distribution of installed capacities (see Appendix A.3) or the covariance matrices, the PCA decomposition offers a more visual and summarising representation of the main trends of variation. Due to their intermittency, integrating more PV panels leads to the installation of other technologies to benefit from free and renewable electricity when it exceeds the electrical EUD. Therefore, we observe that the variation of installed PV is directly linked with the variation of installed industrial electrical resistors and, to a smaller extent, of decentralised and district heating network (DHN) electrical HP. These variations cover the whole transition as the main varying factors given their significant contributions to the PC_1. Where this was an example for correlated technologies, we can also identify some key modal shifts where one technology is either substituted by others or in balance with another one. First, about the LT heat sector, the early stages of the transition, i.e. 2025-2030, sees the shift from mainly decentralised oil and gas boilers towards decentralised and DHN electrical HP. Later in the transition, there seems to be a tight competition between (bio)diesel and fuel cell (FC) trucks that drive the design variance to a smaller extent as they mostly appear in the second and third PCs of the representative years. Not capturing a significant share of variance, there are other modal shifts (e.g. battery electric vehicle (BEV) substituting diesel and gasoline cars) that are not visible through the PCs. Besides these modal

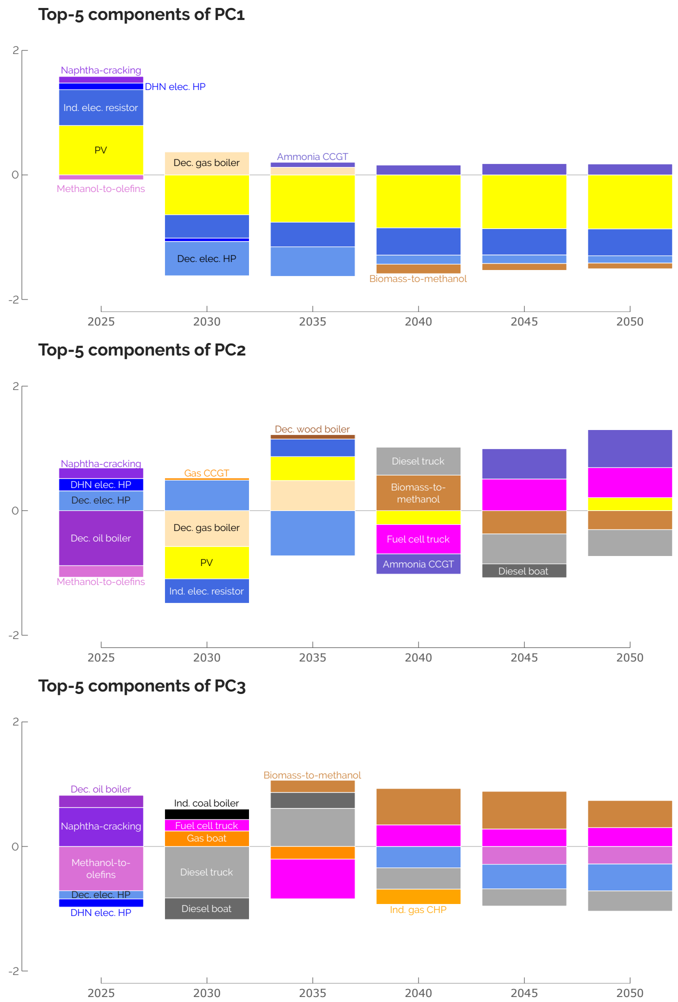

Figure 1.2. Contribution of the top-5 technologies to the first three PCs over the different representative years. Where the variation of photovoltaic (PV) panels supported by the electrification of the HT heat via industrial electric resistors is the main varying drivers over the whole transition, there are tipping years like 2025 for the production of HVC (i.e. naphtha-cracker to methanol-to-olefins (MTO) or 2025-2030 for the production of LT heat (i.e. from oil and gas boilers to electric heat pump (HP).

shifts spread over several representative years, 2025 is the tipping year concerning the shift from naphtha-cracker and methanol-to-olefins to supply HVC. Finally, there are also technologies contributing to PCs because they are the main producing assets of their respective end-use sector and the demand varies significantly, e.g. biomass-to-methanol.

1.1.2 Principal components of the transition

Based on the PCs of each representative year, PC_y, the PCs of the transition, i.e. the metrics to assess the robustness of roadmaps, can be computed. Before aggregating and averaging similar PC_y, it is necessary to rank them to ensure capturing most of the transition variance in the subsequent $PC_{transition}$.

Based on the design variance captured by each PC_y in their respective representative year, we can rank them (see Table 1.2). Summing all of these variances over the different years results in a “pseudo” total variance of the transition. To construct the PCs of the transition, $PC_{transition}$, we keep the PC_y that captures at least 80% of this total variance of the transition (see Section **??**). This results in keeping 11 PC_y: the first PC of each representative year, the second of 2025, 2030, 2035 and 2040 and the third PC of 2025.

Table 1.2. Ranking of PCs per design variance captured in their respective representative year and cumulative share of the captured total variance of the transition

Ranking	**Year**	**PC**	**Design variance** [10^{-4}]	**Cumulative share of total variance** [%]
1	2030	PC_1	61.1	13.9
2	2025	PC_1	55.7	26.5
3	2035	PC_1	52.7	38.4
4	2030	PC_2	38.4	47.2
5	2040	PC_1	33.4	54.7
6	2045	PC_1	26.5	60.7
7	2050	PC_1	22.2	65.8
8	2035	PC_2	20.9	70.5
9	2025	PC_2	19.1	74.8
10	2025	PC_3	15.0	78.2
11	2040	PC_2	8.7	**80.2**
⋮	⋮	⋮	⋮	⋮
34	2050	PC_7	1.6	100

Given the similarity between PC_y, some $PC_{transition}$ result from the aggregation and averaging of the components of several PC_y.

Bibliography

[1] W. E. Walker, R. J. Lempert, J. H. Kwakkel, Deep uncertainty, Delft University of Technology 1 (2012).

[2] O. Castrejon-Campos, L. Aye, F. K. P. Hui, Making policy mixes more robust: An integrative and interdisciplinary approach for clean energy transitions, Energy Research & Social Science 64 (2020) 101425.

[3] G. Limpens, X. Rixhon, F. Contino, H. Jeanmart, Energyscope pathway: an open-source model to optimise the energy transition pathways of a regional whole-energy system, Elsevier in Applied Energy 358 (2024). doi:https://doi.org/10.1016/j.apenergy.2023.122501.

[4] SPF Economie, Vision and strategy hydrogen, October 2022. URL: https://economie.fgov.be/sites/default/files/Files/Energy/View-strategy-hydrogen.pdf.

Appendix A

Pathway optimisation under uncertainties

A.1 Total transition cost

Table A.1 gives the ranking and total Sobol index over the total transition cost of each of the 34 parameters listed in **??**. The first column shows these indicators for the GSA applied on the hourly pathway model. For information, the second column gives the same indicators but for an uncertainty quantification carried out on the monthly pathway model that has some limitations [3] but has the main advantage to run much faster. Given the similar rankings of the parameters between these two, this comparison shows that the monthly model can be a computationally efficient proxy to quantify the uncertainties of the actual hourly model and point out the key parameters on optimisation-driving objective, the total transition cost.

Besides the top-4 parameters, rankings are slightly different. The main difference in terms of ranking relates to the import of electricity from abroad, i.e. its cost of purchasing and its availability. Indeed, as observed by Limpens et al. [3], the monthly model does not require this import given the easier integration of monthly-averaged local variable renewable energy sources (VRES). However, this does not jeopardize the comparative analysis given the similar Sobol' indices. Given their wide range of uncertainty [-64.3%; 179.8%] and their significant role to meet the CO_2-budget, the cost of purchasing electrofuels is the first, by far, impacting parameter. Next, comes, naturally, the industrial EUD, representing, at the nominal value, 60% of the total demands by 2050. The top-3 is completed by the variation of the interest rate, directly impacting the annualisation and the salvage values of the assets. Finally, since the current Belgian whole-energy system deeply relies on fossil resources, and would still do in the near future, the cost of purchasing fossil fuels is part of the impacting parameters. On the contrary, due to the very low annualised, cost, long lifetime leading to a significant salvage value and a low-emitting fuel, the parameters related to small modular reactor (SMR) barely impact the total transition cost.

Table A.1. Total Sobol' indices of the uncertain parameters over the total transition cost in the monthly and hourly pathway models. The similar rankings (and indices) show the validity of using the faster (even though less accurate) monthly model to assess uncertainties over the hourly model.

Parameter	**Ranking (Sobol' index)** Hourly model		Monthly model	
Purchase electrofuels	1	(46.8%)	1	(47.4%)
Industry EUD	2	(23.2%)	2	(23.5%)
Interest rate	3	(12.0%)	3	(11.0%)
Purchase fossil fuels	4	(5.7%)	4	(6.9%)
Variable OPEX of technologies	5	(3.1%)	5	(2.9%)
Purchase biofuels	6	(2.6%)	6	(2.6%)
CAPEX electric motor	7	(2.1%)	8	(1.9%)
Purchase electricity	8	(1.5%)	34	(<0.1%)
Hourly load factor wind turbines	9	(1.1%)	9	(1.3%)
Hourly load factor PV	10	(1.1%)	7	(1.9%)
Potential capacity SMR	11	(0.9%)	11	(0.9%)
CAPEX car	12	(0.8%)	13	(0.7%)
Available local biomass	13	(0.7%)	12	(0.8%)
Passenger mobility EUD	14	(0.7%)	14	(0.7%)
Modal share change LT-heat	15	(0.5%)	15	(0.5%)
Max capacity PV	16	(0.5%)	10	(1.1%)
Households EUD	17	(0.5%)	16	(0.5%)
Services EUD	18	(0.5%)	17	(0.4%)
Max share of public transport	19	(0.3%)	19	(0.3%)
Max capacity onshore wind	20	(0.3%)	18	(0.3%)
CAPEX PV	21	(0.2%)	20	(0.2%)
Efficiency electric motor	22	(0.2%)	22	(0.1%)
Max capacity offshore wind	23	(0.2%)	21	(0.2%)
Available electricity import	24	(0.1%)	33	(<0.1%)
CAPEX ICE	25	(0.1%)	24	(0.1%)
CAPEX fuel cell engine	26	(0.1%)	23	(0.1%)
Efficiency fuel cell engine	27	(0.1%)	25	(<0.1%)
Modal share change freight mobility	28	(0.1%)	26	(<0.1%)
Modal share change passenger mobility	29	(<0.1%)	27	(<0.1%)
CAPEX grid reinforcement	30	(<0.1%)	30	(<0.1%)
CAPEX efficiency measures	31	(<0.1%)	28	(<0.1%)
CAPEX bus	32	(<0.1%)	29	(<0.1%)
CAPEX SMR	33	(<0.1%)	32	(<0.1%)
CAPEX power grid	34	(<0.1%)	31	(<0.1%)

A.2 Imported renewable electrofuels

Table A.2. Comparison of the quantities of imported renewable electrofuels, in TWh, between the REF case, the SMR case and the statistical features from the GSA (i.e. Q1, median and Q3). 2020 is not in the table as, per assumption, no renewable electrofuel is imported for this year. For the sake of clarity, zeroes are replaced by "-".

Year	Case	e-methane	e-hydrogen	e-ammonia	e-methanol
2025	REF	-	-	10	52
	SMR	-	-	10	29
	Q1	-	-	9	2
	Median	-	-	10	47
	Q3	-	-	11	55
2030	REF	-	1	10	52
	SMR	-	1	10	52
	Q1	-	-	9	43
	Median	-	-	10	50
	Q3	-	1	12	57
2035	REF	-	17	10	53
	SMR	-	17	10	53
	Q1	-	-	9	42
	Median	-	5	11	51
	Q3	-	16	33	58
2040	REF	-	16	23	54
	SMR	-	16	10	54
	Q1	-	-	10	41
	Median	-	12	26	51
	Q3	8	16	68	60
2045	REF	40	16	42	54
	SMR	-	16	11	54
	Q1	-	-	12	42
	Median	-	12	37	52
	Q3	35	17	71	60
2050	REF	39	16	44	55
	SMR	7	16	11	55
	Q1	-	-	11	43
	Median	1	13	31	53
	Q3	36	17	66	61

Figure A.1 gives the distribution of the different routes of supply and consumption of gas like methane, hydrogen, ammonia and methanol, resulting from the 1260 samples of the GSA.

Given its lower cost of purchasing than its renewable equivalent (**??**) and lower global warming potential (GWP) than other fossil fuels (i.e. $gwp_{\text{op,NG}} = 0.27\,\text{kt}_{\text{CO}_2,\text{eq}}/\text{GWh}$ versus $gwp_{\text{op,LFO}} = 0.31\,\text{kt}_{\text{CO}_2,\text{eq}}/\text{GWh}$ or $gwp_{\text{op,coal}} = 0.40\,\text{kt}_{\text{CO}_2,\text{eq}}/\text{GWh}$), fossil fossil gas (NG) remains the main source of gas in the system until 2040. Besides bio-hydrolisis as the main consumer of wet biomass to consistently produce gas, e-methane eventually substitutes fossil natural gas by 2045-2050 in order to respect the CO_2-budget for the transition. Its versatility makes gas used by a wide variety of technologies in the different sectors. Initially, in 2020, decentralised gas boilers, combined cycle gas turbine (CCGT) and industrial gas boilers represent the biggest consumers of gas with 39%, 21% and 16% of the total consumption, respectively. Progressively, in line with the rest of the system shifting towards more efficiency in the mid-term, industrial combined heat and power (CHP) represent the lion's share, next to other usages in the transport or LT-heating sectors.

On the contrary, import of fossil-based hydrogen, largely produced from steam-methane-reforming [4], is rarely part of the solution due to the emissions related to the consumption of natural gas. E-hydrogen is the consistent source of hydrogen in the system, next to local production (i.e. steam-methane-reforming, electrolysis or ammonia-cracking) in some rare cases where low industrial EUD coincides with more abundant electricity from SMR or PV. In terms of consumption, FC-trucks are the more consistent player. FC-cars are also at stake but in specific cases where their CAPEX and the CAPEX of electric vehicles are in the bottom and the top of their respective uncertainty range.

Becoming cheaper than its fossil equivalent at early stages of the transition (i.e. from 2030 onward), e-ammonia is the exclusive stream of ammonia in the system, except rare cases. Then, on top of its consistent non-energy demand (NED), the largest consumption of ammonia is CCGT as flexible power generation units, to substitute their e-methane equivalents that have a higher levelised cost of energy (LCOE) (**??**).

Similarly to ammonia, on top of local production in rare cases, e-methanol is the key source for methanol. Besides its own NED, methanol is mostly consumed to produce HVC via the MTO process instead of naphtha-cracking, in order to respect to CO_2-budget for the transition.

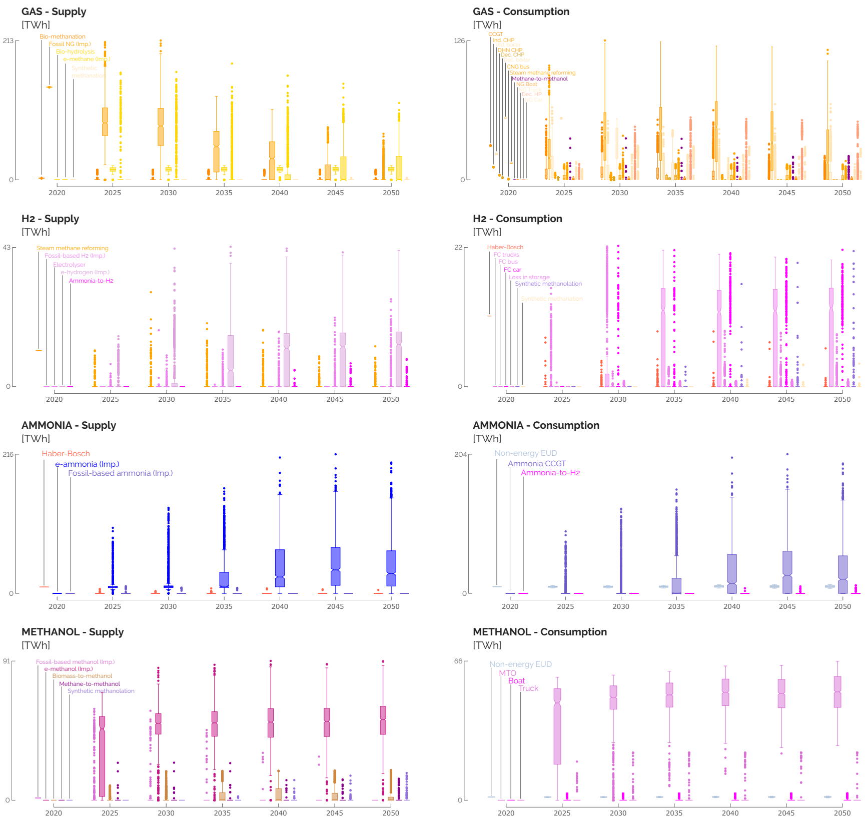

Figure A.1. Distribution of the different streams of supply (left) and consumption (right) of gas, hydrogen, ammonia and methanol from the global sensitivity analysis (GSA).

A.3 Installed capacities

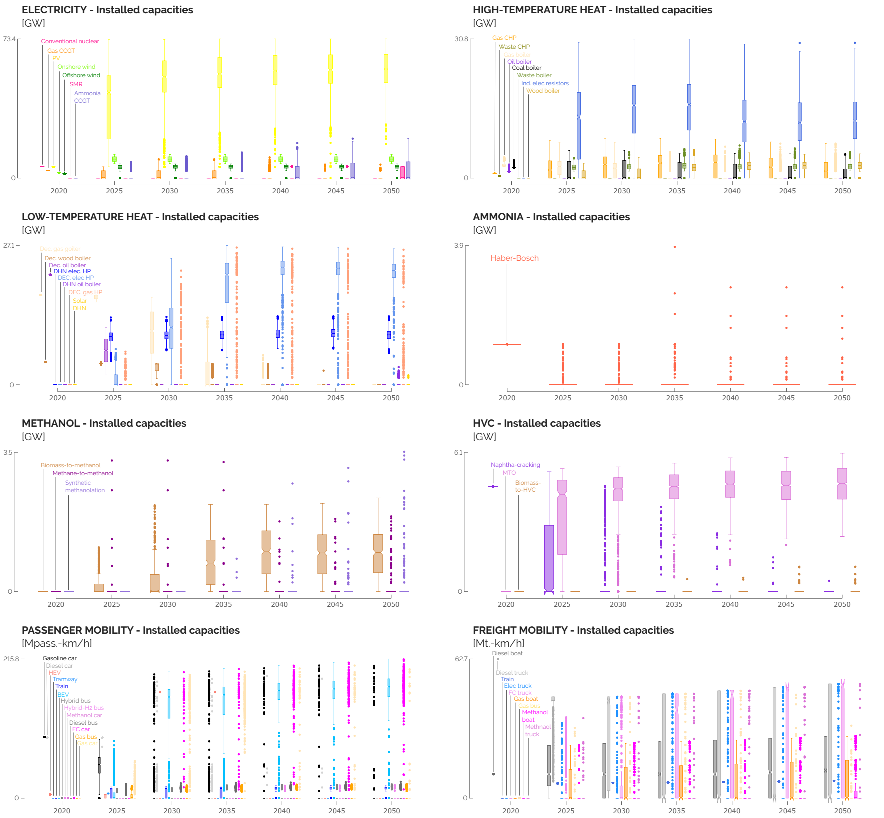

Figure A.2. Distribution of the installed capacities among the different end-use sectors from the global sensitivity analysis (GSA).